Supplementary Methods

All SEM imaging, EBSD and Raman analyses were carried out at the ISAAC analytical facility at the School of Geographical and Earth Sciences, University of Glasgow.

EBSD and Raman set up:

For EBSD analyses we used a FEI Quanta 200F field emission scanning electron microscope (SEM) equipped with an EDAX TSL Hikari high speed EBSD camera running Orientation Imaging Microscopy (OIM) software version 5.32. Samples were highly polished (down to 0.06 μm) and coated with approximately 5 nm of carbon, and analysed in high vacuum mode with a beam aperture of 50 μm and an accelerating voltage of 20 kV. The Kikuchi patterns were indexed using the American Mineralogist Crystal Structure (AMCS) database.

Raman analyses were carried out with a Renishaw Invia Raman Microscope with Wire 3.2 software. Initially, reference spectra for Direct Classical Least Squares (DCLS) mapping were collected using a 514 nm laser excitation source at 100% laser power (10 accumulations, 2 second exposure time). A spectral range of 113.35 to 1140.75 cm^{-1} was obtained by static scans with a centre of 830 cm^{-1}. The baseline of each spectrum was subtracted to allow better comparison of the bands detected. Mapping (Raman imaging) was carried out using StreamLine Plus using a 50× objective (spatial resolution = 1.3 μm) and an exposure time of 5 seconds. Using DCLS, the raw mapping data were partitioned into distinct aragonite and calcite maps.

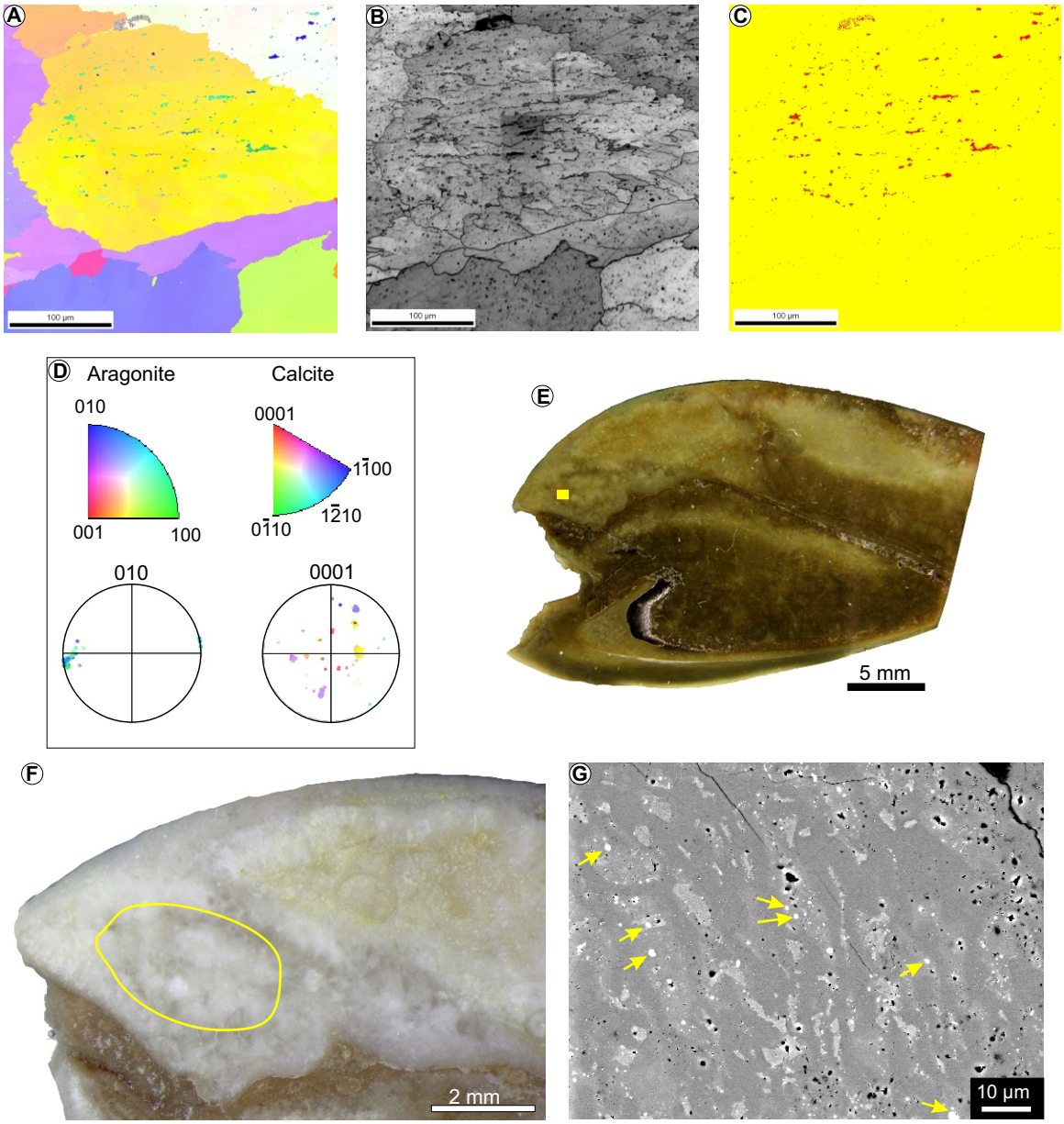

Suppl. Figure DR1. *Trimerella ekwanensis* from the Hudson Bay lowlands (Attawapiskat Formation); A – C: EBSD results (not cleaned): A: crystallographic orientation, B: diffraction intensity (higher diffraction intensity in B correlated with brighter greys), and C: phase maps (yellow = calcite, red = aragonite). D. Color code for crystal orientations in fig. A and pole figure of calcite and aragonite crystals figured in fig. 1 (pole figure contains only points with a consistency index above 0.1); note that all aragonite 'islands' cluster together. E. Reflected light image of the sample used for EBSD; yellow box indicates approximate position of analyzed area. F. Reflected light image of posterior part of shell with yellow line highlighting the approximate extent of aragonite in this specimen. G. SEM backscatter image showing the general appearance of the aragonite (yellow arrows) in this specimen. All images from ROM 61155.

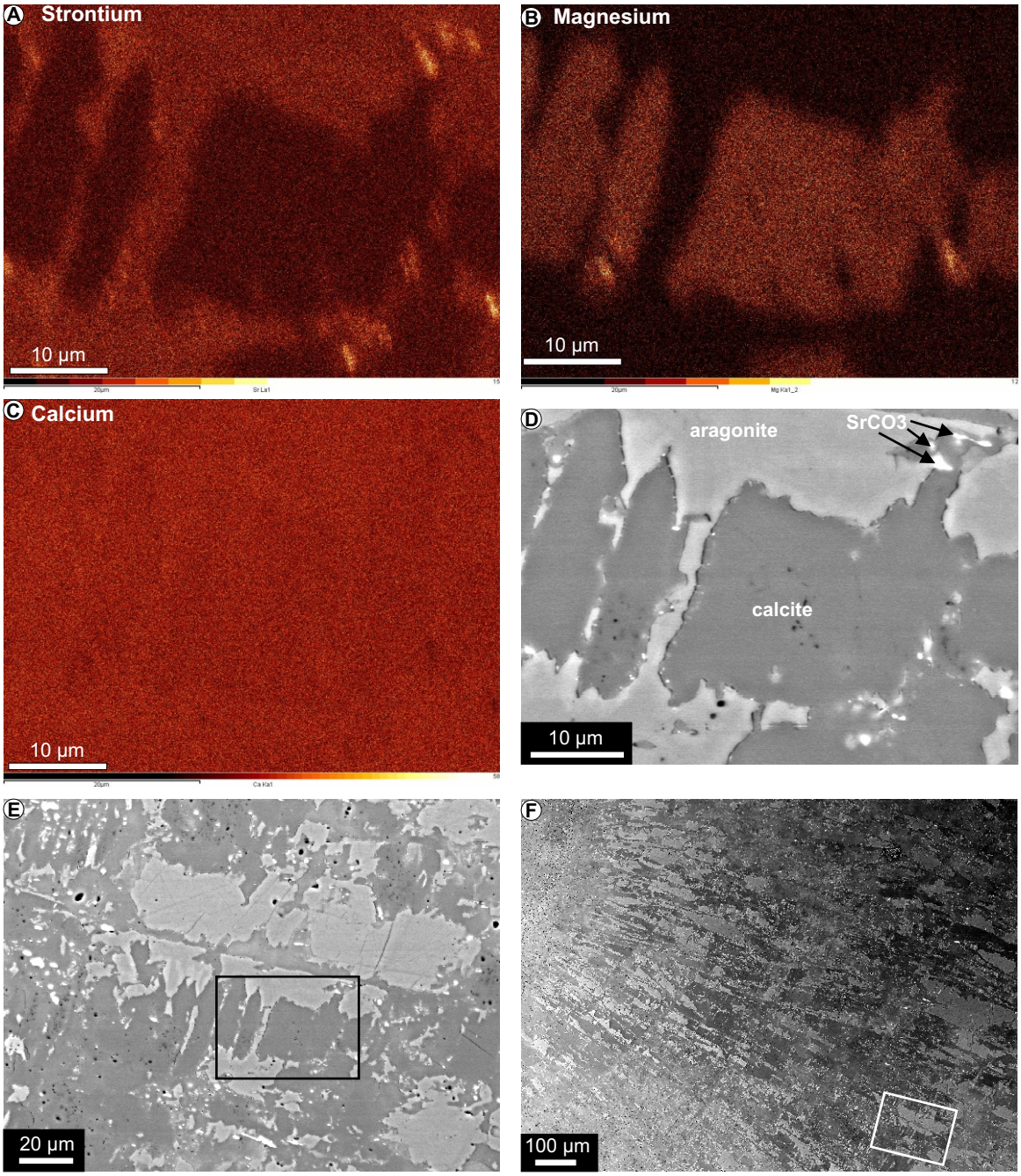

Suppl. Figure DR2. *Trimerella* sp. From Gotland, Slite Formation; A – C: Elemental maps of strontium, magnesium and calcium. D. SEM backscatter image of the same area as A-C showing aragonite, calcite and small granules of strontionite ($SrCO_3$). E. Backscatter SEM image with position of D indicated by box and showing the fragmented nature of the aragonite. F. Backscatter SEM image showing the position of E (white box). All images from PMU 1234/1.

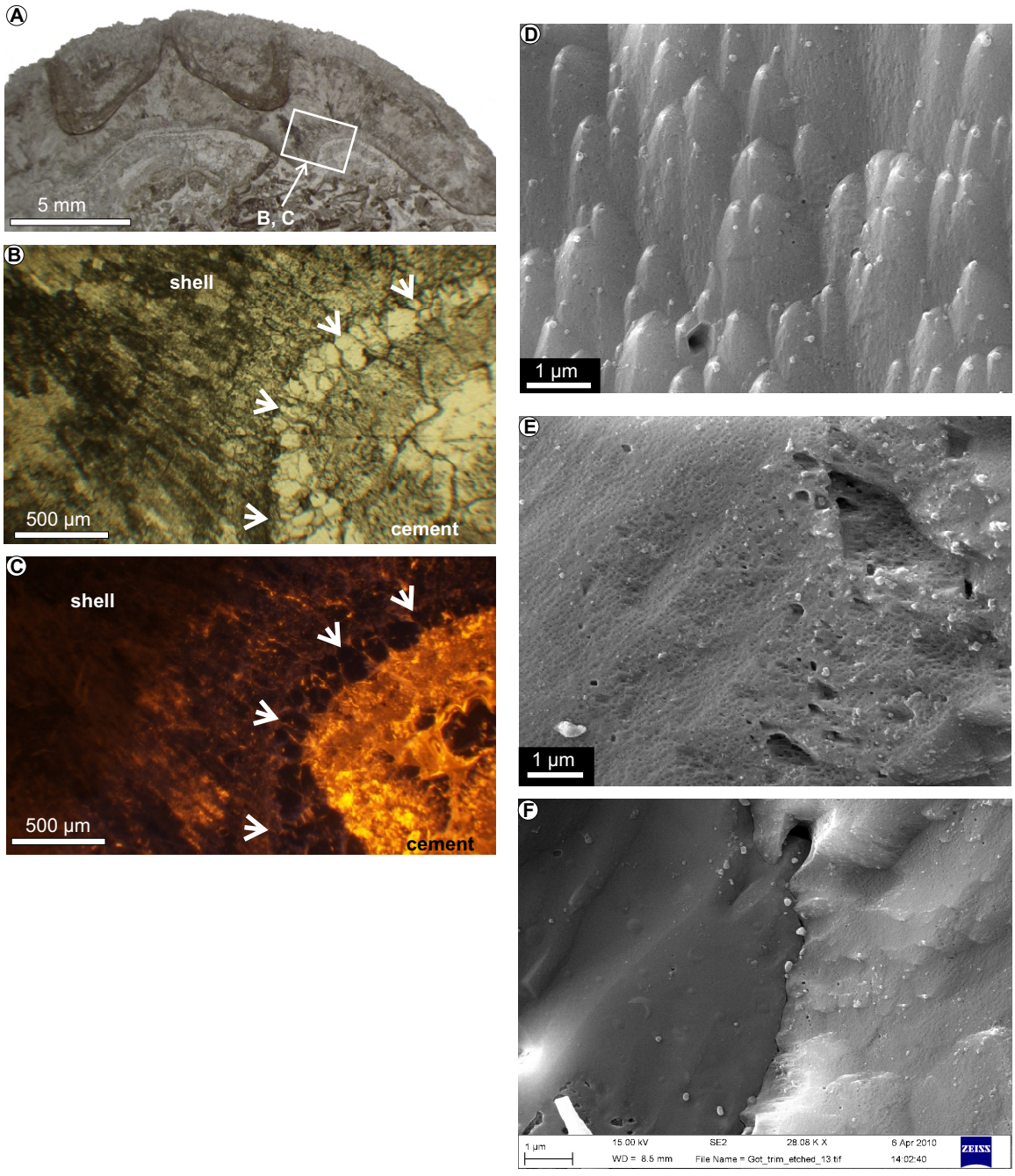

Suppl. Figure DR3. All images of *Trimerella* sp. from Gotland, Slite Formation; A. Transmitted-light image of thin section through shell and matrix; box shows position of figures B and C. B. Detail of A showing the contact between the shell and the underlying cement; arrows indicate inner shell margin. C. Petrographic cathodoluminescent image of the same area as fig. B showing localized luminescence along the shell margin, non-luminescent early calcite cement and a strongly luminescent later calcite cement; arrows indicate inner shell margin. D - E. SEM images of etched aragonite (whole image) showing pronounced nano-porosity and inclusions. F. SEM image of etched aragonite (right half – with numerous nano-pores) and calcite (left half – smooth appearance). Figs. A-C: PMU 1234/2; Figs. D-F: PMU 1234/1.

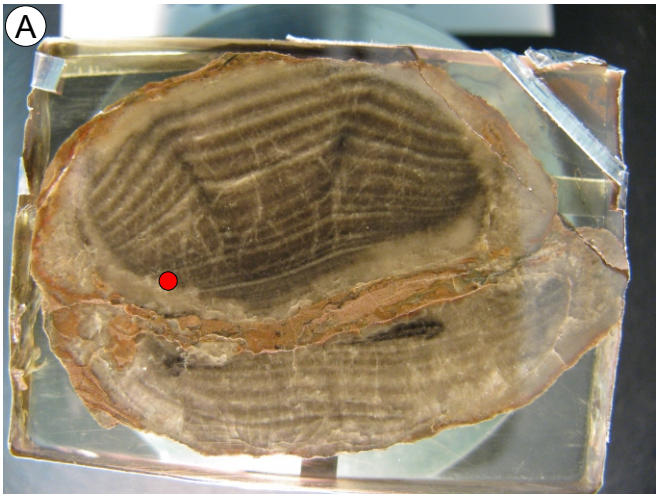

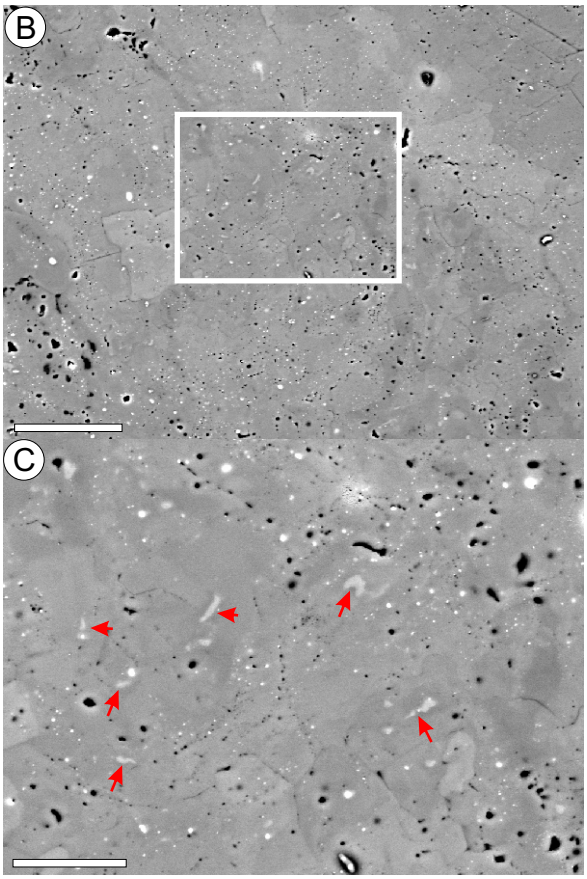

Eodinobolus stevensi
Fossil Hill Limestone
Australia
Upper Ordovician

MMF44975

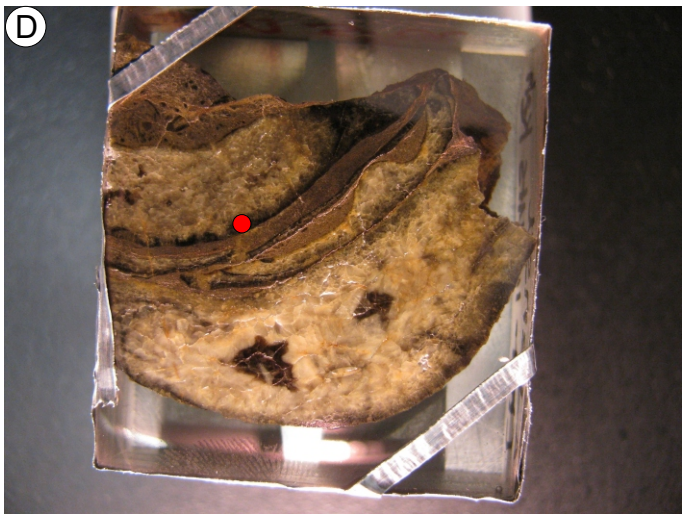

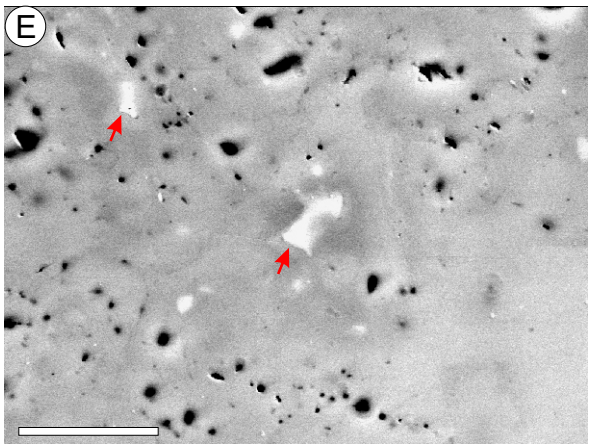

Adensu monstratum
Chu-Ili Mountains, Kazakhstan
Upper Ordovician (Katian)

NMW 98.28G.1999

Suppl. Figure DR4. A and D: Photos of polished and gold-coated specimens in resin blocks (red point shows position of figures B-C and E, respectively); B-C: BSE images of A; box in B shows position of C; E: BSE image of D; red arrows point to aragonite inclusions. Scale bars are: B: 50 µm, C: 20 µm, E: 10 µm.

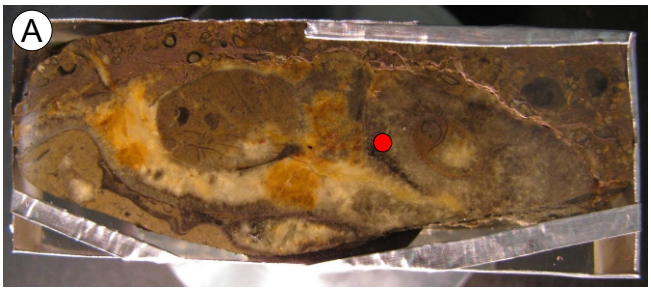

Keteiodoros bellense
Dripstone Formation
Australia
Wenlock (Silurian)

GLAHM 131708

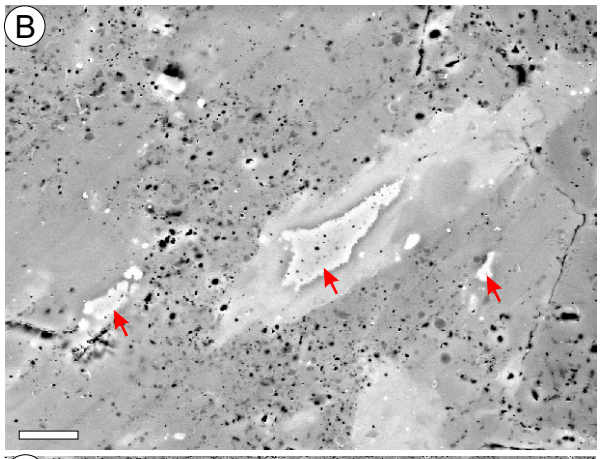

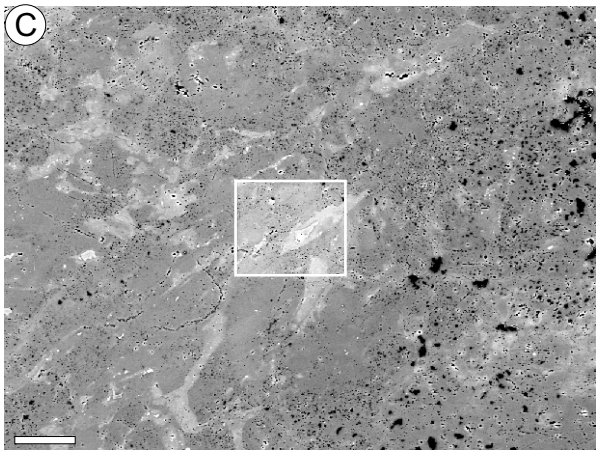

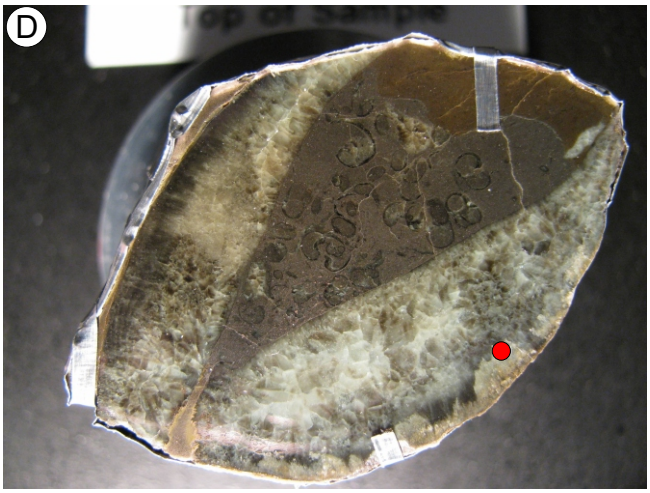

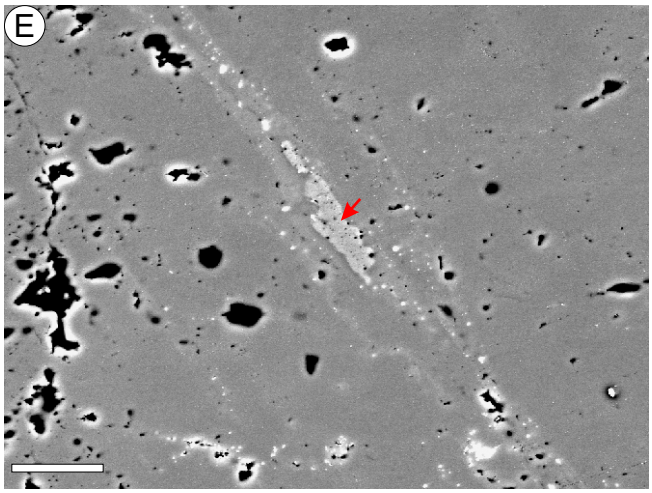

Eodinobolus stevensi
Fossil Hill Limestone Formation
Australia
Upper Ordovician

GLAHM 131709

Suppl. Figure DR5. A and D: Photos of polished and gold-coated specimens in resin blocks (red points show positions of figures B-C and E, respectively). B-C: BSE images of A; box in C shows position of B; E: BSE image of D; red arrows point to aragonite inclusions; Scale bars are: B = 10 µm, C = 50 µm, E = 20 µm.

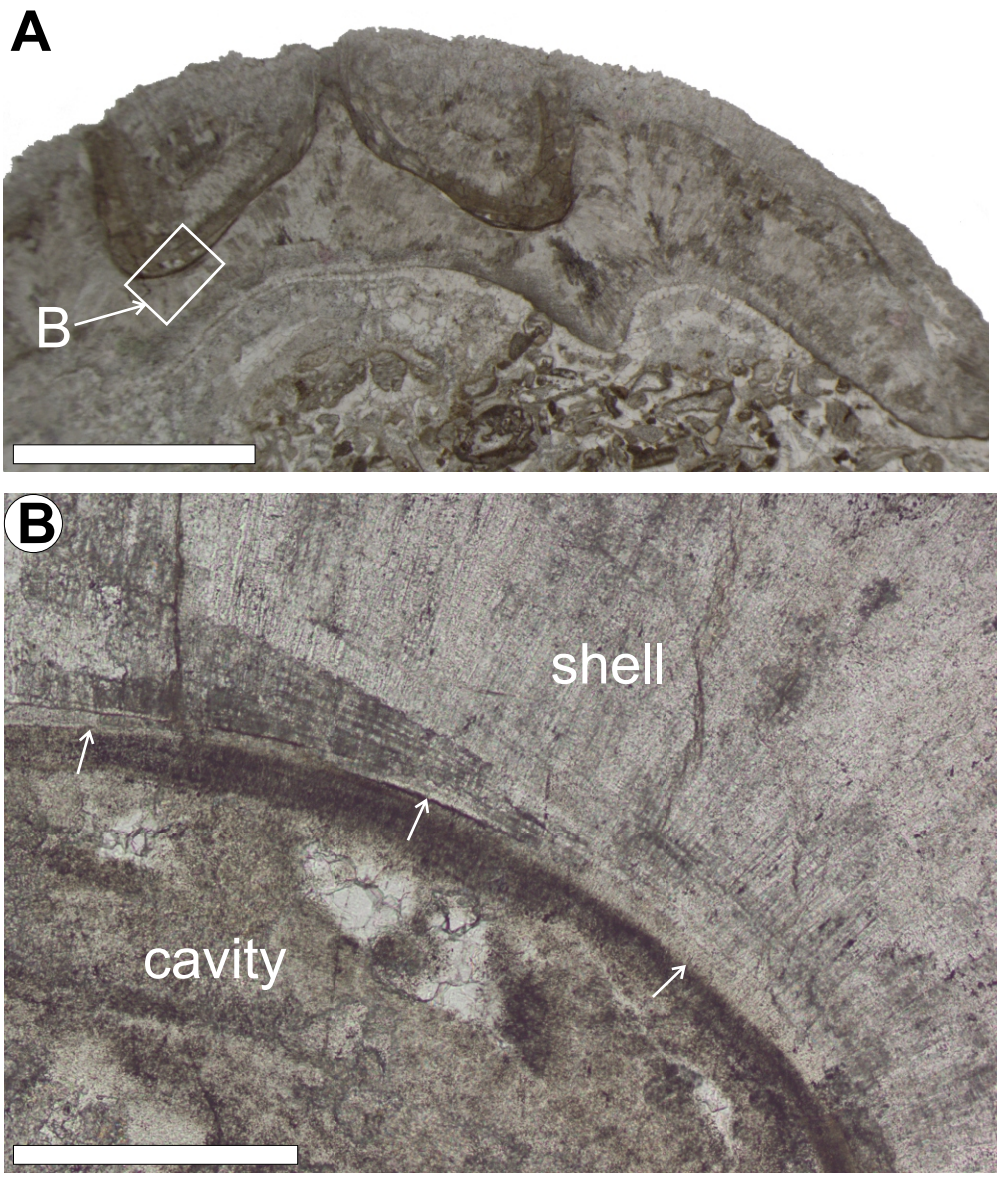

Suppl. Figure DR6. Microstructure of aragonite in *Trimerella* sp. from Gotland (same sample as figure 1 in the paper); transmitted light photographs of thin sections of the counterpart of the polished surface used for EBSD and Raman mapping. Boxed area shows position of figure B; PMU 1234/2. B. Transmitted light photograph showing the border (arrows) between the shell and cement; PMU 1234/2. scale bars are: a = 5 mm, b = 0.5 mm.

1 = Hudson Bay lowlands
Attawapiskat Formation
lower Llandovery
Silurian - ca. 10 Ma younger

2 = Gotland, Sweden
Slite Formation
Wenlock
Silurian - ca. 15 Ma younger

3 = Chu-Ili Range, Kazakhstan
Dulankara Formation
lower Katian
Ordovician - ca. 10 Ma older

4 = New South Wales, Australia
Fossil Hill Limestone
lower Katian
Ordovician - ca. 10 Ma older

5 = New South Wales, Australia
Dripstone Formation
Wenlock
Silurian - ca. 15 Ma younger

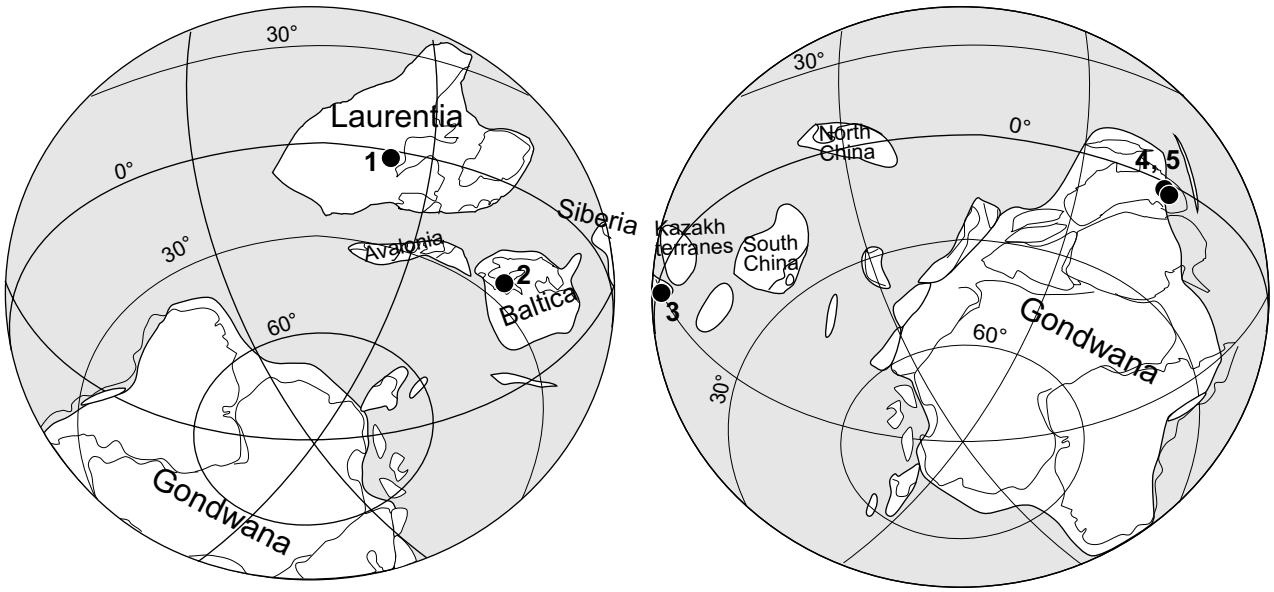

Suppl. Figure DR7. Paleogeographic map of the early Silurian (440 Ma) showing the distribution of the studied aragonite-bearing samples. The stratigraphic age of the samples with respect to the map date of 440 Ma is given in the legend above the map. Relative position of the major Early Paleozoic continents for the early Silurian is mainly after Cocks and Torswik, 2002, Journal of the Geological Society, v. 159; p. 631-644.